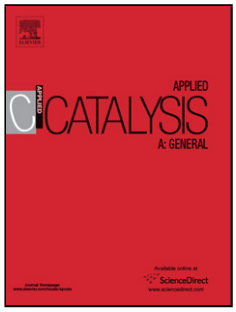

Title: Copper-Gold Nanoparticles Encapsulated Within Surface-Tethered Dendrons as Supported Catalysts for the Click Reaction

Authors: Aibolat Koishybay, Daniel F. Shantz

PII: S0926-860X(18)30330-2
DOI: https://doi.org/10.1016/j.apcata.2018.07.007
Reference: APCATA 16733

To appear in: *Applied Catalysis A: General*

Received date: 2-4-2018
Revised date: 18-6-2018
Accepted date: 3-7-2018

Please cite this article as: Koishybay A, Shantz DF, Copper-Gold Nanoparticles Encapsulated Within Surface-Tethered Dendrons as Supported Catalysts for the Click Reaction, *Applied Catalysis A, General* (2018), https://doi.org/10.1016/j.apcata.2018.07.007

Copper-Gold Nanoparticles Encapsulated Within Surface-Tethered Dendrons as Supported Catalysts for the Click Reaction

Aibolat Koishybay and Daniel F. Shantz*

Department of Chemical and Biomolecular Engineering, Tulane University, 6823 St. Charles Avenue, New Orleans, LA 70118, United States. Email: dshantz@tulane.edu

Graphical Abstract

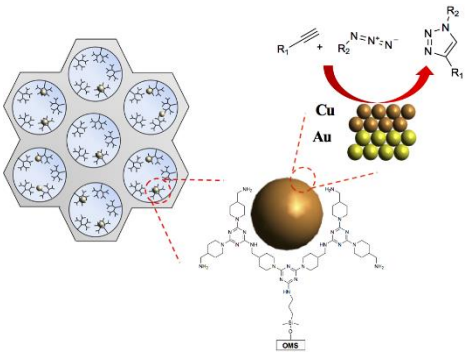

Koishybay and Shantz Highlights

- 1. Stable copper overlayers on gold nanoparticles were synthesized
- 2. Better catalytic activity observed than unsupported CuNPs in the click reaction
- 3. Copper leaching was less than CuNPs encapsulated on bare SBA-15
- 4. Intermediates can be studied by in-situ FTIR

Keywords. Hybrid materials, dendrons, copper-gold nanoparticles, click chemistry

Abstract

The synthesis, characterization, and catalytic testing of copper and copper:gold nanoparticles in melamine-based dendrons supported on SBA-15 is reported. It was found that by first making small gold nanoparticles using the dendrons as templates, stable copper(0) overlayers could then be successfully deposited. These samples were used as catalysts for the click reaction, with the most active samples possessing rates of 8.9 mol triazole produced/(mol copper – hour), nearly 50 times high than literature reports of copper nanoparticles in solution. In constrast, the gold nanoparticles themselves are inert for this reaction, consistent with the copper being deposited as an overlayer on the gold nanoparticles. Copper leaching was shown to be less pronounced for particles formed in the dendrons versus copper simply deposited on SBA-15. Larger dendrons lead to suppressed rates due to diffusion resistance with rates decreasing from 8.9 to 5.2 to 0.69 mole triazole produced/(mole Cu-hour) for G1, G2, and G3 respectively. Infrared spectroscopy was used to monitor the reaction in real time, and provided information about the various surface intermediates formed.

1. Introduction

Ordered mesoporous silica (OMS) has enjoyed a wide range of interest as a catalyst/catalyst support in innumerable investigations.[1-3] This is a result of the OMS possessing a high surface area and highly uniform and tunable pore sizes. OMS has been used in many applications, including both the synthesis of supported metal nanoparticles as catalysts on OMS as well as being used as a support for tethering organometallic complexes.[4-10] There has also been substantive research in the growth of polymer brushes off the surface of mesoporous silicas. The contribution the Shantz lab has made to this area is the synthesis of melamine based dendrons using amine-functionalized SBA-15 as a support.[11-14] Our initial report coincided with a similar report from the Alper and Al-Sayari lab of PAMAM dendrons grown off mesoporous silicas.[15] This has been a promising area of research both for our labs, as well as other labs following up on our initial discovery.

There have been numerous studies that are well reviewed in the literature reporting metal nanoparticles formed in OMS either from bare OMS or OMS functionalized with simple groups such as aminosilanes.[16, 17] The synthesis of surface-tethered organometallics and how those materials compare to their homogeneous counterparts has also been reported and well-reviewed.[7, 18, 19] An area that has received less attention, is the synthesis of metal nanoparticles on OMS materials that have been surface functionalized with more complex ligands such as polymers and dendrons. The ability to generate hybrid materials with both the function of a metal and an organic moiety will be potentially of interest in a range of problems including selective capture and conversion schemes as well as cascade or domino reaction schemes. To that end our lab is investigating the feasibility of growing uniform metal nanoparticles in the surface-tethered melamine dendron materials we have reported previously.[11-13, 20-22]

There are numerous literature studies forming metal nanoparticles in dendrons in solution, or so called dendrimer encapsulated nanoparticles (or DENs). This approach was pioneered by the Crooks lab in the late 1990s using metals such as palladium, gold, copper, and platinum.[23-28] Those works showed the

ability to use the dendrimer as a template to make uniform nanoparticles. Subsequent work from the Crooks lab and other have expanded this work to a wide range of metals as well as the formation of bimetallic nanoparticles.[15, 28-32] These works in part served as an inspiration for recent work forming palladium nanoparticles in melamine dendrons[22] as well as the current work to determine if such an approach would be as successful for forming supported copper nanoparticles.

Alkyne-azide cycloaddition or so called click reaction is an elegant approach to the synthesis of 1,4-disubstituted 1,2,3-triazoles that have a wide range of applications, such as organic chemistry, material science, polymer science and medicinal chemistry.[33-37] The click reaction continues to garner much interest because it is a highly efficient and reliable reaction that runs in mild conditions with high regioselective yields, allows connection of a wide range of functional groups and involves straightforward product isolation procedures.[38-40] Click chemistry primarily evolved around homogeneous Cu(I) catalysts which limit industrial chemical and pharmaceutical applications due to the challenges related to the catalyst removal, recovery, reuse as well as toxic Cu contamination of products.[38, 41] Heterogeneous catalysis is an alternative that can overcome these drawbacks.[41-44] Bulk copper was proposed as an alternative for homogeneous Cu(I) catalysts but the use of CuNPs proved to be more efficient. However, unsupported CuNPs have some limitations such as rigorous CuNP synthesis steps, aggregation, high temperatures, use of commercially unavailable reagents and use of stabilizing agents that add to the cost.[45] Therefore, the use of supported CuNPs promises to be advantageous and is the focus of this study.

2. Experimental

*2.1 General***.** Tetraethoxysilane (TEOS, ≥99%, Alfa Aesar), hydrochloric acid solution (HCl, 2.0N, BDH), and Pluronic P123 (PEG-PPG-PEG, MW = 5800, Sigma-Aldrich) were used in the SBA-15 synthesis. 3-aminopropyldimethylethoxysilane (APDMTES, Gelest) was used for aminosilane grafting. ACS grade toluene was obtained from BDH. It was dried in an MBraun solvent purification system and stored over activated molecular sieves (Alfa Aesar, 3A, 3-5mm beads) to remove residual water. Cyanuric

chloride (CC, ≥98, Alfa Aesar), tetrahydrofuran (THF, ≥99.9, no stabilizer, EMD Millipore), N,N-diisopropylethylamine (DIPEA, ≥99%, Sigma-Aldrich), methanol (BDH, ACS grade), dichloromethane (DCM, BDH, ACS grade), 4-(aminomethyl)piperidine (AMP, ≥96%, Sigma-Aldrich), and anhydrous piperazine (PIP, ≥99%, Alfa Aesar) were used in the dendrimer synthesis. Copper(II) chloride dihydrate (Baker Analyzed, ACS Reagent), sodium borohydride (≥99.99%, Sigma-Aldrich) and gold(III) chloride trihydrate (≥99%, Sigma-Aldrich) were used for the metal loading experiments. Benzyl azide (≥94%, Alfa Aesar), cyclohexylacetylene (≥98%, Alfa Aesar) and triethylamine (≥99%, Sigma-Aldrich) were used in the click reaction. Deuterated chloroform with +0.03% v/v tetramethylsilane (TMS) was obtained from Cambridge Isotope Laboratories and used for the NMR analysis of the click reaction. THF, DCM and toluene were dried prior to use with an MBraun solvent system. All other chemicals were used as received.

2.2 SBA-15 synthesis. SBA-15 samples were synthesized using the method reported by Zhao et al.[46] As an example, 20 g of Pluronic P123 was dissolved in 125 mL of deionized water and 600 mL of 2 M HCl by stirring for 5 h at room temperature. Then, 42.5 g (45.5 mL) of TEOS was added to the solution and stirred for 24 h at 35 °C. The mixture was then aged at 80 °C for 24 h under static conditions. The reaction product was collected by vacuum filtration, washed with deionized water and air-dried overnight. The Pluronic was removed by calcination. The sample was heated from room temperature to 100 °C at a rate of 1 °C/min, then held at 100 °C for 2 hours, then the temperature increased from 100 °C to 550 °C at a rate of 1 °C/min, and finally held at 550 °C for 8 h.

2.3 Amine-functionalization of SBA-15. Amine-functionalized SBA-15 was synthesized *via* post-synthetic amine grafting. Typically, 1.0 g of calcined SBA-15 was mixed with 0.5 mmol (94 μL) APDMTES in 100 mL of anhydrous toluene. The mixture was stirred at room temperature for 24 h. The solid product was collected by filtration, washed with copious amounts of toluene and methanol, and air dried overnight.

2.4 Synthesis of dendron-SBA-15 hybrid materials. Dendron hybrid materials were synthesized per prior work.[11-13, 22] As an example, 4-aminomethylpiperidine (AMP) dendrons were made by adding 1.0 g of amine-functionalized SBA-15 to 25 mL of a 0.3M cyanuric chloride in THF solution and 2.5 mL of DIPEA. The mixture was stirred for 24 h at room temperature in a closed container. The reaction products were collected by filtration and washed with methanol, DCM and THF, respectively. The solid product was then mixed with 25 mL of a 0.4 M AMP in THF solution and stirred for 24 h at room temperature. The sample was again filtered and washed with methanol, DCM and THF, respectively. This sample was denoted as G1-AMP-SBA-15. Higher generation samples were synthesized by repeating the procedure stated above one or two times to obtain G2-AMP and G3-AMP dendrimers, respectively (Scheme 1). To synthesize piperidine (PIP) containing dendrons, 25 mL of 0.4 M PIP in THF solutions were used instead of 0.4 M AMP solutions. Throughout samples are denoted as Gx-AAA-SBA-15 where x is the dendron generation and AAA is either AMP for dendrons containing 4-aminomethylpiperidine as the diamine or PIP for dendrons containing piperidine as the diamine.

2.5 Metal–dendron SBA-15 materials. Copper and gold loading on dendron-SBA-15 was performed by dispersing 0.6 g of Gx-AAA-SBA-15 in 2.6 mL of 0.025 M $HAuCl_4$ solution. The mixture was stirred for 10 min before gold was reduced with fivefold excess of a 50 mM aqueous solution of $NaBH_4$. The solid product was separated by centrifugation and washed with deionized water. The obtained material was dispersed in 6 mL of 0.032 M $CuCl_2 \cdot 3H_2O$ solution

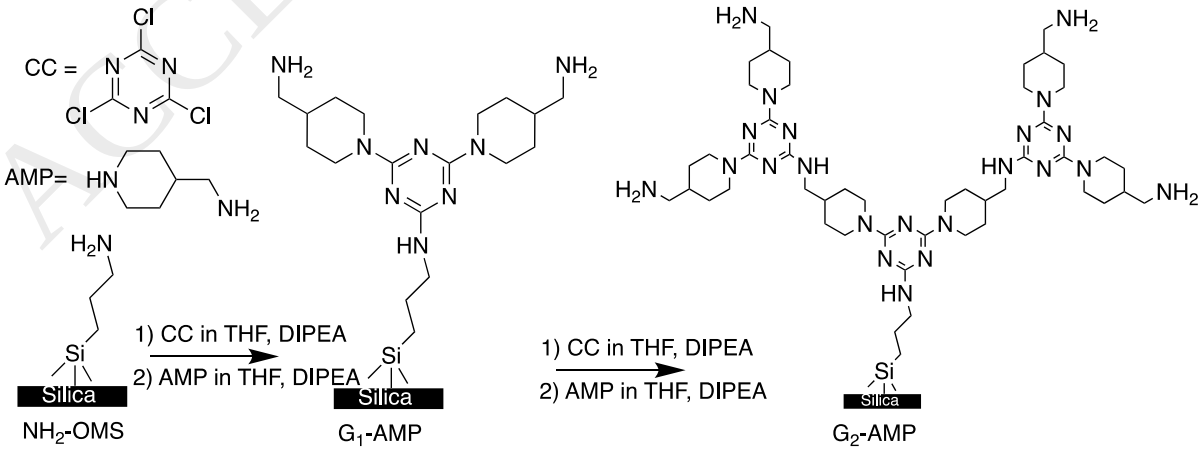

Scheme 1. Synthesis of dendrons illustrated with G2-AMP.

and stirred for another 10 min before it was reduced with a fivefold excess amount of 50 mM aqueous solution of $NaBH_4$. The final product was collected by filtration, washed several times with deionized water, dried in a Schlenk flask under vacuum at room temperature and labeled as Xwt% Cu_YAu-Gx-AAA-SBA-15 where X, Y, Gx and AAA are weight percent loading of copper, copper to gold molar ratio, dendrimer generation and dendron type, respectively. As an example, a second-generation AMP dendron with two weight percent copper and a copper to gold molar ratio of 3 is denoted as 2wt% Cu_3Au-G2-AMP-SBA-15.

2.6 Analytical. Powder X-ray diffraction (PXRD) measurements were performed using a Rigaku MiniFlex 600 diffractometer with CuKα radiation over a range of 20–80° 2θ. For SBA-15, the measurement was performed from 0.5–4° (2θ). In the case of SBA-15, the instrument background at a low angle (< 1° 2θ) was subtracted by measuring a zeolite ZSM-5 material (MFI, pure silica) over the same range. Attenuated total reflection Fourier-transform infrared (ATR-FTIR) measurements were performed on a Nicolet iS50R spectrometer. Diffuse reflectance ultraviolet-visible (UV-vis) spectroscopy measurements were performed using an Evolution 300 instrument equipped with a diffuse reflectance stage. Barium sulfate was used as the reference standard. Thermal gravimetric analyses (TGA) were performed using a TA Instruments Q500 over a temperature range of 25–600 °C using air as a carrier gas and a temperature ramp rate of 1 °C min^{-1}. Nitrogen adsorption experiments were performed using a Micromeritics ASAP 2020 with approximately 100 mg of sample. The samples were degassed under vacuum at 150 °C for 24 h before analysis. The mesopore volumes and surface areas were determined using the α_s-method. The mesopore size distributions were calculated from the adsorption branch of the isotherms using the Barrett–Joyner–Halenda (BJH) method with a modified equation for the statistical film thickness. X-ray photoelectron spectroscopy (XPS) experiments were performed using a VG Scientific MKII system with a Mg Kα X-ray source. The pressure in the chamber during analysis was < $5x10^{-8}$ mbar. Peak fitting was performed with a custom VBA program in Microsoft Excel using Voigt

profiles together with a Shirley background function. Transmission Electron Microscopy (TEM) and Scanning Transmission Electron Microscopy (STEM) measurements were performed using a FEI Tecnai G2 F30 Twin with Oxford EDS, Gatan Imaging Filter and EEL Spectrometer. The samples were dispersed in 95% ethanol solution with sonication for 1 min and deposited on carbon-coated Cu grids (200 mesh, Electron Microscopy Science) and the solvent was evaporated. All ^{1}H NMR spectra were collected on a Bruker Avance 500 MHz using $CDCl_3$ as a solvent and TMS as an internal standard.

2.7 Reaction monitoring with IR. Infrared spectroscopy measurements were performed using a flow cell setup inside a Bruker-Vertex 70 FT-IR instrument. The measurement parameters were 2 cm^{-1} resolution and 30 scans. The measurements were performed with a room temperature DLaTGS detector. The reaction mixture was prepared by dispersing 0.033 g of catalyst, which corresponds to 5 mol% of Cu per 1 mole of reactant in 10 mL of THF. 0.2 mmol of triethylamine was added to the solution and subtracted as a background. 0.2 mmol of benzyl azide and 0.2 mmol of cyclohexylacetylene were added to the reaction mixture and heated to 50 ^{o}C. The reaction progress was recorded every 20 min.

2.8 Catalytic testing. The click reaction (scheme 2) was carried out as follows. Unless noted otherwise, two mmol of benzyl azide, 2 mmol of cyclohexylacetylene and 2 mmol of triethylamine were added to 0.16 g of catalyst, which

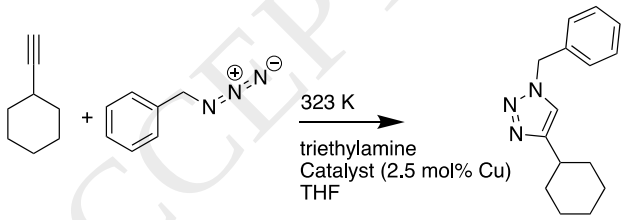

Scheme 2. Cycloaddition of benzyl azide to cyclohexyl acetylene.

corresponds to 2.5 millimoles of copper per 100 millimoles of reactant in 4 mL of THF. The reaction mixture was then heated to 50 °C and the reaction conversion was monitored by ^{1}H NMR. At different intervals, 100 μL of the reaction mixture was transferred into a small centrifuge tube and the solid catalyst was removed from the solution by centrifugation at 13800 xg for 3 min. The liquid was diluted with 750

μL of deuterated chloroform and analyzed by ^{1}H NMR at 25 °C. Conversion was calculated by integrating the peaks for the 1-benzyl-4-cyclohexyl-1H-1,2,3-triazole (s 7.16 ppm, 1H, CH) and (s, 2H, CH_2) product with respect to that of the benzyl azide (s 4.35 ppm, 2 H, CH_2) and cyclohexylacetylene (d 2.04–2.05 ppm, 1 H) peaks. Note that in all experiments performed there were no side products observed.

3. Results and Discussion

3.1 General Characterization. The dendron-SBA-15 hybrids, prior to metal uptake, were characterized using a battery of methods to validate that the target dendrons were formed on the SBA-15 surface. X-ray diffraction, nitrogen porosimetry, thermal gravimetric analysis, and infrared spectroscopy (Figures S1-S8, Supporting Information) are all consistent with prior work from our lab. The supports are well-ordered SBA-15 materials, the textural properties change as expected as upon increasing the dendron generation, the target groups are present and that the ligand loading is consistent with prior work showing the vast majority of the organic fragments in fact have the dendron structure shown in Scheme 1.

*3.2 Copper nanoparticle formation***.** Recent work from our lab demonstrated the ability to form small (< 2 nm), uniform palladium nanoparticles on G2-PIP-SBA-15 materials.[22] Expanding on that work, the synthesis of small copper nanoparticles on PIP-SBA-15 and AMP-SBA-15 materials was explored. As an initial control copper was loaded onto SBA-15 and reduced. In that case, PXRD confirmed the presence of copper(0) particles, however the copper species formed were large (> 10 nm) and generally found by STEM to not be in the SBA-15 mesopores. In contrast, attempts to make copper(0) particles on PIP-SBA-15 samples led to smaller particles. However, PXRD, XPS, and diffuse-reflectance UV-Vis measurements showed that the copper was not exclusively copper(0), and that over the span of a few days of storage the fraction of oxidized copper increased significantly. By contrast, using AMP dendrons supported on SBA-15 it was possible to make Cu(0) nanoparticles based on PXRD; however these samples suffered from stability and tended to oxidize. It was not possible to form pure, stable Cu(0) nanoparticles in the dendrons.

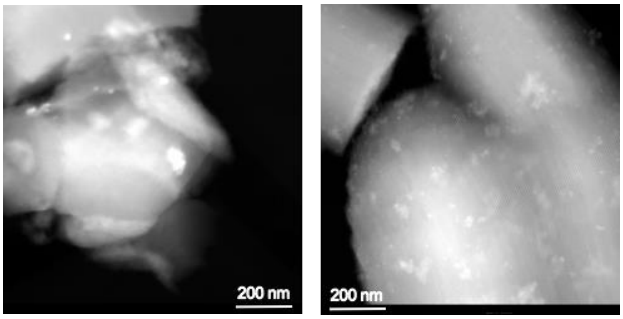

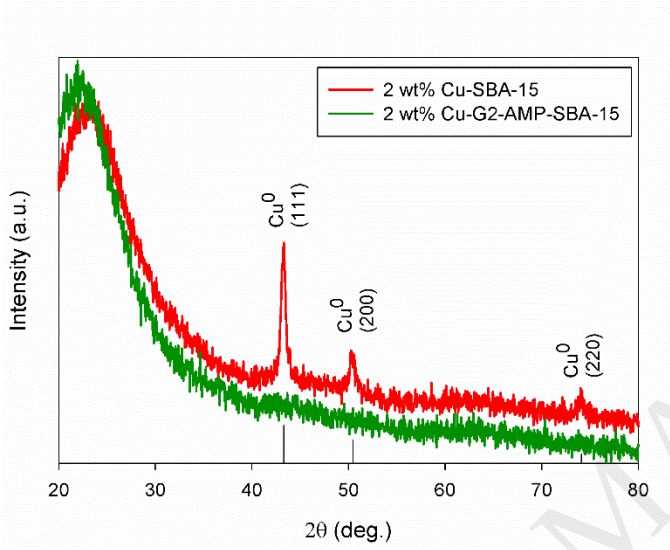

Figure 1. STEM images of 2wt% Cu-SBA-15 (top left) and 2wt% Cu-G2-AMP-SBA-15 (top right. (Bottom) PXRD patterns of the samples.

3.3 Copper-gold nanoparticles. The above results highlight the challenges of forming stable, small copper(0) nanoparticles in dendrons. This was in contrast to our previous work using palladium where it was found one could obtain stable Pd(0) 2 nm particles in dendrons. Given prior literature that indicated one route to stabilizing copper(0) was to overlayer it onto gold this was attempted.[47-49] Figure 2 shows PXRD results for samples containing 1 wt% Cu and a 3:1 molar ratio of copper:gold on G2-AMP-SBA-15. The sample where the two elements were reduced simultaneously resulted in large domains of gold based on the results in Figure 2 (red trace). The sample where gold was added and reduced then, followed by copper addition and reduction (blue trace), by contrast resulted in small nanoparticles based on PXRD. The same phenomena was seen for samples where the addition order was reversed, i.e. copper addition then reduction, followed by gold addition and reduction (black trace). In this last sample the

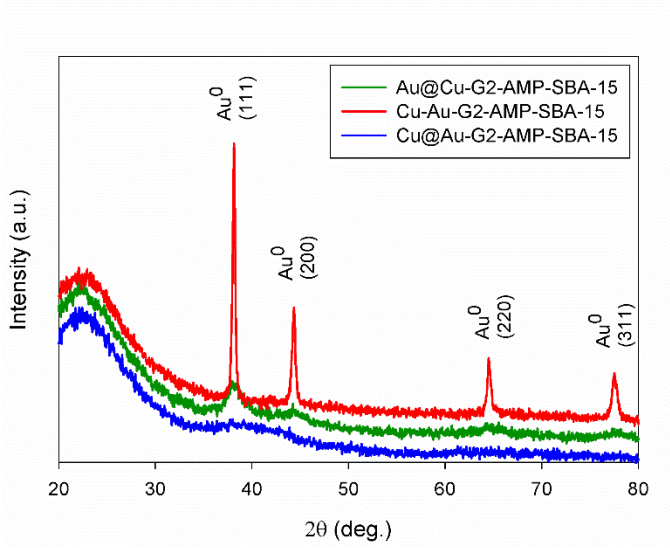

Figure 2. Effect of reduction sequence on copper / gold bimetallic systems at one weight percent copper and 3:1 Cu:Au molar ratio on a G2-AMP-SBA-15 sample. Red trace simultaneous reduction of copper and gold. Black trace, sequential addition and reduction of copper then gold. Blue trace, sequential addition and reduction of gold then copper.

diffraction peaks for gold could be observed but were dramatically broader. None of these samples exhibited features consistent with the presence of copper oxides or large copper(0) domains. The effect of dendron generation and Cu:Au ratio at a fixed copper loading were also explored. In all cases, no copper oxide species are observed by PXRD. As the generation of dendron increases the gold domain size decreased based on PXRD and as the amount of gold in the copper:gold system increased an increase in the intensity of the gold peaks, but not a decrease in the peak widths, was observed in PXRD (Figures S9-S10). These results are consistent with the picture that gold(0) nanoparticles can be used to stabilize the presence of copper(0) species. Further evidence for this was found by XPS (Figure 3) and UV-Vis (Supporting Information Figure S11) which did not give any indication for the presence of oxidized copper.

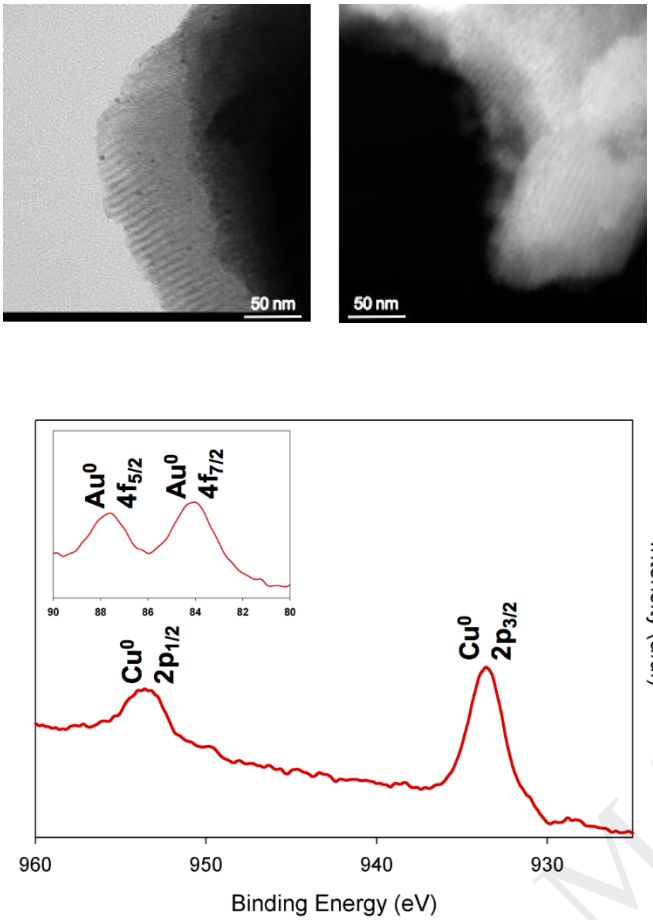

Figure 3. (Top left) TEM and (top right) STEM images of CuNP inside SBA-15 mesopores. (Bottom) XPS spectrum of 2wt%-Cu_3Au-G2-AMP-SBA-15.

3.4 Click reaction. The copper:gold samples described above were investigated for the coupling of an alkyne with an azide, i.e. click chemistry. Control measurements indicated that bare SBA-15, G2-AMP-SBA-15, and 2 wt% Au-G2-SBA-15 gave no conversion of the reactants after 24 hours at 323 K. 2wt% Cu-SBA-15 was active for this reaction with a conversion of 94% after 18 hours at 323 K, which corresponds to an approximate rate at short reaction times (< 5hrs) of 4.3 mol triazole produced/(mol copper-hour). 2 wt%-Cu-G2-AMP-SBA-15 was also screened for this reaction, and gave an 81% conversion after 24 hours of reaction at 323 K. These results are consistent with prior literature that shows copper is active for the click reaction, and that gold is not.[35] With this information in hand the Cu-Au materials were tested.

Figure 4 shows catalytic data for the Cu-SBA-15, 2 wt%-Cu-G2-AMP-SBA-15, and 2 wt% Cu_3Au-G2-AMP-SBA-15. The Cu_3Au sample was more active than the Cu-G2-AMP sample. This was consistent with our characterization work that suggested the copper formed an effective overlayer on the gold, i.e. we effectively realized higher copper utilization as the same amount of copper in the Cu_3Au sample was being overlaid onto the gold versus forming pure

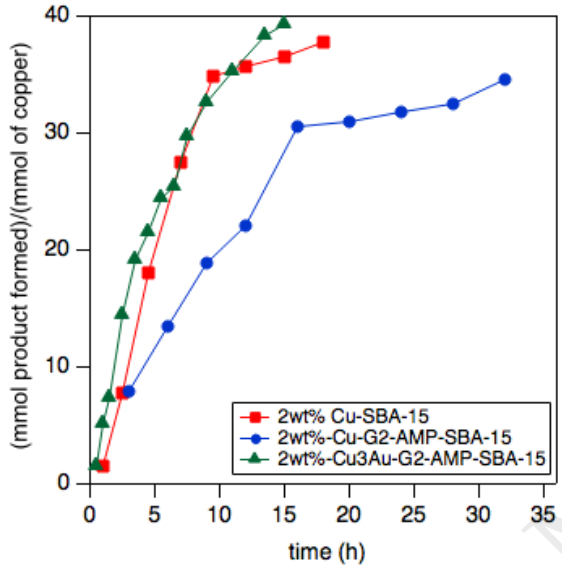

Figure 4. Catalytic results for 2wt%-Cu-SBA-15, 2wt%-Cu-G2-AMP-SBA-15, and 2wt%-Cu_3Au-G2-AMP-SBA-15.

copper particles. In the case of the Cu_3Au sample the early time data gives an estimated rate of 5.2 mol triazole produced/(mol Cu – hour). For comparison, comparable conditions were used by Alonso and coworkers with copper nanoparticles[50] and gave rates in the range of 0.001 to 0.04 mol triazole produced/(mol Cu-hour). Thus our samples are notably more active on a copper basis. That the Cu-SBA-15 sample was more active than the Cu-G2-AMP-SBA-15 sample could have two explanations. The first is that for Cu-SBA-15 more copper was leached into solution, and thus both homogeneous and heterogeneous catalysis were being observed. The second is that there was more diffusion resistance in the case of the G2-AMP sample. It is likely that both factors are at work, but we did not attempt to uncouple their relative contributions. Leaching studies of the samples are described in more detail below.

3.4.1 The effect of the copper:gold ratio. Figure 5 shows the catalytic results for samples with Cu:Au ratios of 1:1, 3:1, and 5:1 (XRD and STEM of 5:1 and 1:1 samples in Support Information, S12 and S13). As can be seen the 1:1 and 3:1 samples were

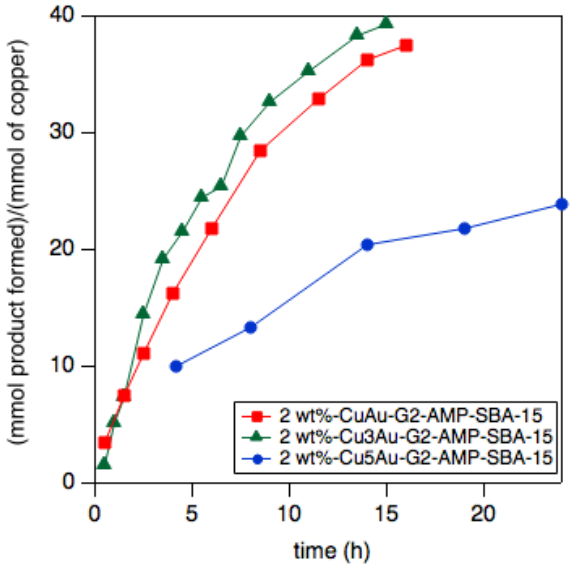

Figure 5. Effect of the Cu:Au ratio at a given copper weight loading in G2 dendrons on the catalytic properties of the samples. All three samples contain two weight percent copper.

comparable. The 5:1 sample showed decreased reactivity on a copper normalized basis. A simple explanation for this finding is that upon increasing the copper to gold ratio that thicker layers of copper were being formed on the gold particles, leading to a lower utilization, i.e. a smaller fraction of the copper atoms were on the surface of the nanoparticles. Qualitative calculations indicate that to coat a 2 nm gold particle that an approximately 1:1 Cu:Au ratio is needed, consistent with our findings in figure 5 and our conclusion of an overlayer. Two additional controls were performed to test this idea. The first was to make copper nanoparticles followed by addition and reduction of gold. In this case the conversion was only 17% after 24 hours. The second was to take a 2wt%-Cu_3Au-G2-AMP-SBA-15 sample and anneal it at 150 °C under nitrogen to form the intermetallic[51], with no change in the particle size observed by STEM or PXRD. In that case the conversion declined from 98% at 15 hours to 80% at 24 hours (71% at 12 hours) after annealing. Both of these control experiments support our hypothesis that the copper

formed an overlayer on the gold, and that the enhanced reactivity observed was a result of higher copper utilization, and not due to changing the electronic properties of the copper. This was explored more thoroughly using infrared spectroscopy (*vide infra*).

3.4.2 The effect of the dendron generation. A series of 2wt%-Cu_3Au-Gx-AMP-SBA-15 samples of different dendron generation were synthesized (STEM in Supporting Information, S13). As can be seen in Figure 6 there is a systematic decrease in the rate on a normalized copper basis when going from G1 to G2 to G3. Estimates of the rates for these samples based on the early time data are 8.9 to 5.2 to 0.69 mole triazole produced/(mole Cu-hour) for G1, G2 and G3 respectively. This same trend was observed in prior work in our lab using these dendrons without

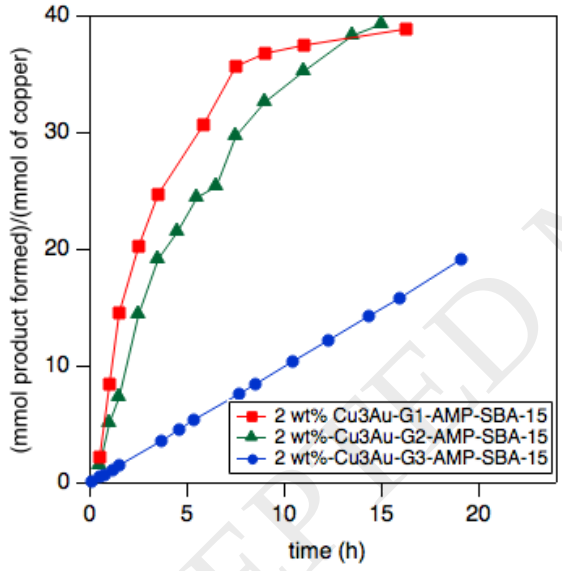

Figure 6. Effect of dendron generation on the observed rate for a series of 2wt%-Cu3Au-AMP-SBA-15 samples.

metals as catalysts for the Nitroaldol reaction. This finding was ascribed to the increase in diffusion resistance as one goes to larger dendrons, and again consistent with prior work a more substantive change was seen in going from G2 to G3 than from G1 to G2.

3.4.3 Catalyst Stability and Metal leaching. The stability of our CuAu-catalysts was also studied (Table S3 and Figures S14-S17 in Supporting Information). Two sets of recycle studies for the 2wt% Cu_3Au-G2-AMP-SBA-15 were performed. The first studies used a 17.5 h on stream interval. In this case the conversions went from 96% to 71% (first recycle) to 7% (second recycle). In the second set of experiments a reaction time of 24 hours was used. In that case the conversion went from 100% to 48% to approximately 1% for the fresh catalyst, first recycle, and second recycle. Characterization of the spent catalyst points to two causes for this deactivation. The first was fouling of the catalyst. TGA analysis of the sample after two 24 hour reaction cycles showed a weight loss of 33% for the G2 sample, whereas the weight loss due to dendrons was 22% for the sample before catalytic testing. This finding shows that organic matter deposits on the catalyst during reaction. The second cause for deactivation was metal leaching and subsequent homogeneous catalysis by copper. To probe this the hot filtrate method was employed. Table one summarizes the results obtained for three samples

Catalyst	Conversion	
	Click reaction @ 50 °C for 6 hours	Hot filtrate after 12 hours post separation @ 50 °C
2wt% Cu-SBA-15	64 %	93 %
2wt% Cu-G2-AMP-SBA-15	39 %	49 %
2wt% Cu_3Au-G2-AMP-SBA-15	62 %	76 %

Table 1. Summary of conversion before and after catalyst separation.

wherein the conversion was measured at six hours, the catalyst separated from the reaction, and the filtrate heated for an additional twelve hours. As can be seen the Cu-SBA-15 had the most metal leaching based on the increase in conversion, and has effectively the same conversion as determined after 18 hours when the SBA-15 sample was not separated. The dendron samples, both 2wt% Cu-G2-AMP and 2wt% Cu_3Au-G2-AMP, had some leaching though the increase in conversion after separation of the catalyst was smaller than for the copper SBA-15 material. Additional, EDS of the spent catalyst (Supporting Information) shows that while the parent material has the proper copper to gold ratio, after reaction the catalyst no longer contains gold, and has a slightly reduced copper content. Thus under reaction conditions the gold leaches, resulting in a material similar to the copper supported dendron sample which

according to table 1 shows some copper leaching via the hot filtrate test. In regards to the state of the copper, XPS and XRD before and after testing only show the presence of Cu(0). UV-Vis is somewhat more ambiguous as the changes are subtle but could be interpreted as the presence of mixed oxidation state copper.

3.5 Infrared spectroscopy. The results above demonstrated that the materials made were catalytically active for the click reaction. IR was chosen to follow the reaction and develop deeper insights into the reaction, with two specific aims. The first aim was to observe the kinetics and any intermediates in the catalytic cycle to see if our system was similar/different to homogeneous copper. The second aim was to try and further validate our hypothesis that we were forming copper ovelayers and simply observing improved rates due to higher efficiency of the copper, i.e. the reactivity variations did not have an electronic effect origin.

Figure 7 shows the time resolved IR data for the Cu_3Au sample. The feature at 3257 cm^{-1} is due to the alkyne (**1**), the feature at 2094 cm^{-1} is due to the azide (**2**), and the feature at 1780 cm^{-1} is due to the triazole (**5**). There are two additional features, one at 2337 cm^{-1} due to an intermediate bound to copper (**3**), and a feature at 1727 cm^{-1} that is due to the bound product (**4**). The results in Figure 7 indicate that IR can be used to follow the reaction in real time. Variations

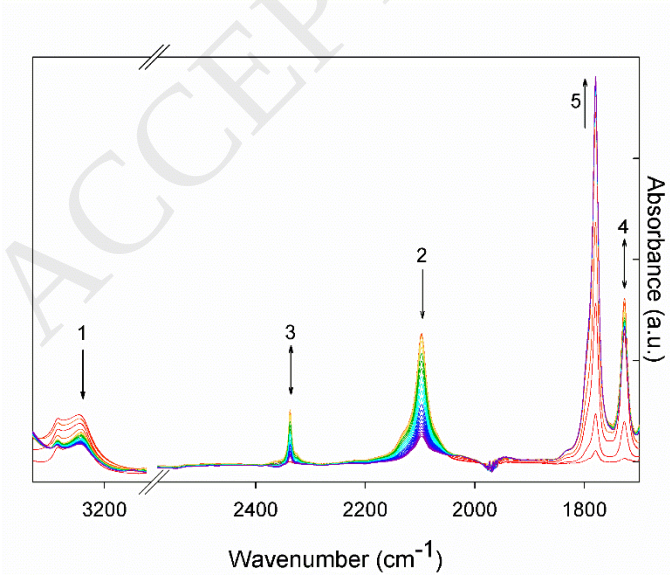

Figure 7. Time resolved IR data for 2wt% Cu_3Au-G2-AMP-SBA-15 catalyzed click reaction.

of the ratio of the alkyne and azide, i.e. 2:1 or 1:2 versus 1:1, appears to make little or no difference in the intensity evolution of the IR spectrum (Figure S18). The results indicate that the alkyne adsorbs rapidly, there is an induction period before azide consumption is observed, and we believe that the formation of the intermediate prior to ring closure and triazole formation is the rate limiting step.

Figure 8 shows our putative mechanism for this reaction, and Figure 9 shows normalized absorbance as a function of the reaction time extracted from the results in Figure 7. There are a few important observations from the results in Figure 9. First, the triazole product absorbance saturates at very low conversion (the conversion determined for these experiments is less than 2% in all cases). Second, as mentioned above, it is clear that an appreciable amount of the alkyne rapidly adsorbs on the copper

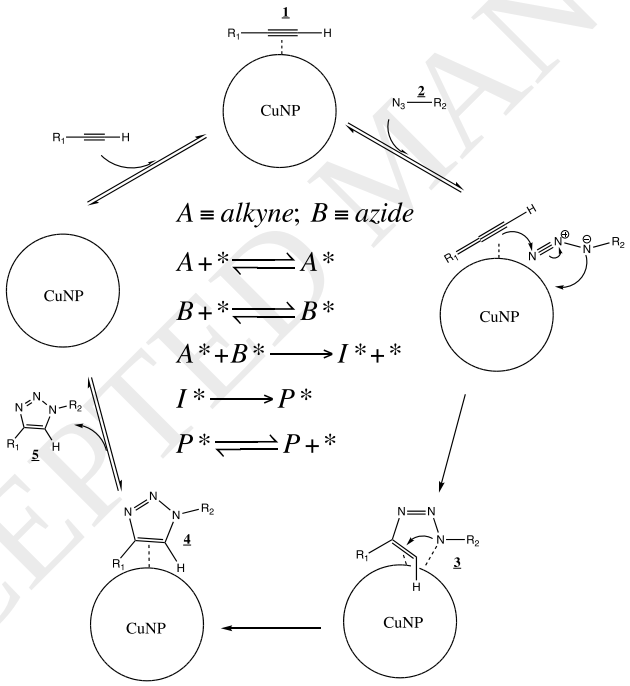

between when the

Figure 8. Putative mechanism for the click reaction.

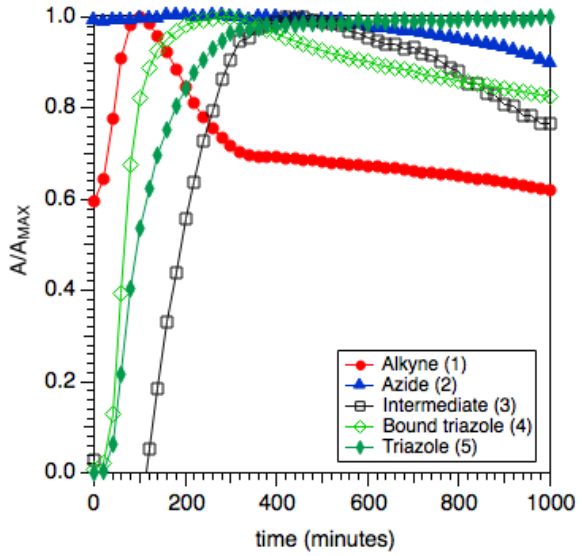

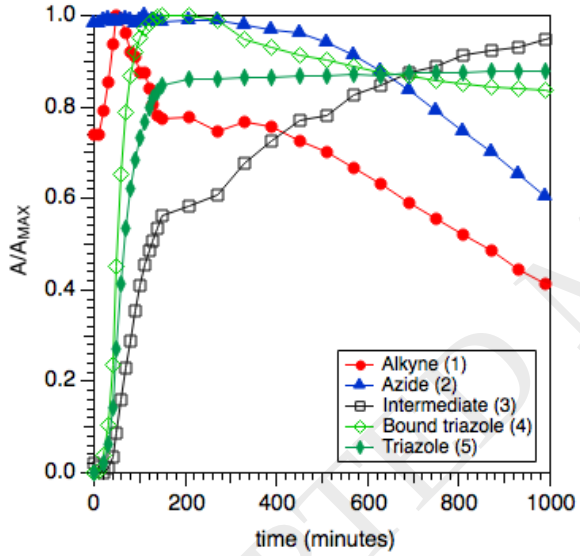

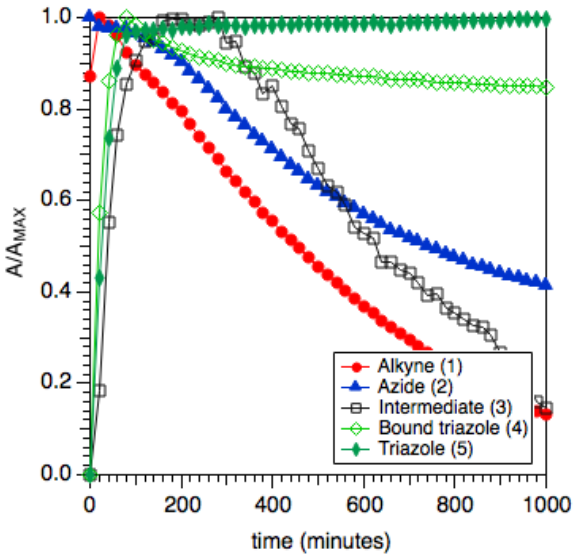

Figure 9. Normalized IR absorbance profiles as a function of reaction time for the (top) CuAu, (middle) Cu_3Au, and (bottom) Cu_5Au G2-AMP-SBA-15 samples.

reaction mixture is prepared and the experiment started (5-10 minutes). Third, as the copper to gold ratio increases the azide and alkyne absorbances decrease more quickly. Finally, at a copper to gold ratio of three the maximum in the surface intermediate (**3**) takes much longer to occur than the other ratios. The reason for this last point is unclear. The IR spectra for the CuAu and Cu_5Au samples are included in the Supporting Information (Figure S19). Efforts were made to fit the absorbance versus time data (both normalized and un-normalized) based on the mechanism shown in Figure 8, however it was not possible to properly capture the measured profiles. Some possible complications include large differences in the absorbance of the products and intermediates versus the reactants. That the triazole product plateaus (i.e. saturates) in the IR data at very low conversion is consistent with this. Consistent with this we found in separate experiments that under the conditions employed low concentrations of triazole (5 mM) led to non-linearities in the absorbance, i.e. we were outside the beer's law limit. Despite this, the IR clearly allowed us to track the reaction and observe intermediates that have been observed previously in the homogeneous catalysis click chemistry literature. That all samples including a G2-AMP-SBA-15 (not shown) displayed very similar trends in the IR is consistent with our hypothesis that overlayering the copper on gold does not lead to dramatic changes in the electronic properties of the copper.

4. Conclusions

The synthesis, characterization, and catalytic testing of copper and copper:gold nanoparticles in melamine-based dendrons supported on SBA-15 was reported. The key to controlling the oxidation state of the copper was to form overlayers of copper on gold nanoparticles as evidenced by ultraviolet visible spectroscopy and X-ray photoelectron spectroscopy. Regarding the catalytic properties of these materials, copper:gold ratios of three to one and lower were found to be preferred for catalysis. Copper leaching was shown to be less pronounced for particles formed in the dendrons versus copper simply deposited on SBA-15. The various controls performed were consistent with the picture of the synthetic approach depositing copper overlayers on gold. Infrared spectroscopy provided information about the various surface intermediates formed consistent with prior literature mechanisms from homogeneously copper catalyzed click reaction studies. The current works shows the metal-dendron hybrids to be promising catalysts for this reaction and offers design strategies for building complex materials for use in heterogeneous catalysis.

5. Acknowledgments

We gratefully acknowledge Professor Russ Schmehl and S. L. Guertin at Tulane for access to the IR spectrometer useful discussions. The IR instrument was acquired through support from the Louisiana Board of Regents award TR_24_2014-ENH-TR-25. D.F.S. gratefully acknowledges partial support from Entergy and Tulane University.

6. Supporting Information.

Powder X-ray diffraction (PXRD) patterns of parent SBA-15, nitrogen adsorption isotherms, TGA results, and IR spectra of the PIP and AMP SBA-15 samples investigated. PXRD patterns of Cu:Au 3:1 AMP samples, PXRD patterns of G2-AMP samples with varying Cu:Au ratios, UV-Vis of 2wt% Cu_3Au G2-AMP-SBA-15 sample, STEM of 2wt% Cu_5Au and CuAu – G2-AMP-SBA-15 samples, STEM of the G1 and G3 2wt%-Cu_3Au-AMP-SBA-15 samples. EDS, PXRD, XPS, UV-Vis and IR spectra of 2wt%-Cu_3Au-AMP-SBA-15 sample before and after the click reaction. Time resolved IR data for the 2wt%

Cu_3Au-G2-AMP samples with varying and azide:alkyne ratios and for the 2wt%-CuAu-G2-AMP-SBA-15 sample and 2wt%-Cu_5Au-G2-SBA-15 sample.

7. References

[1] J.S. Beck, J.C. Vartuli, W.J. Roth, M.E. Leonowicz, C.T. Kresge, K.D. Schmitt, C.T.W. Chu, D.H. Olson, E.W. Sheppard, S.B. McCullen, J.B. Higgins, J.L. Schlenker, A New Family of Mesoporous Molecular-Sieves Prepared with Liquid-Crystal Templates, J. Am. Chem. Soc., 114 (1992) 10834-10843.
[2] U. Ciesla, F. Schüth, Ordered Mesoporous Materials, Micropor. Mesopor. Mat., 27 (1999) 131-149.
[3] W. Li, D.Y. Zhao, An overview of the synthesis of ordered mesoporous materials, Chemical Communications, 49 (2013) 943-946.
[4] R.K. Sharma, S. Sharma, S. Dutta, R. Zboril, M.B. Gawande, Silica-nanosphere-based organic-inorganic hybrid nanomaterials: synthesis, functionalization and applications in catalysis, Green Chemistry, 17 (2015) 3207-3230.
[5] K. Moller, T. Bein, Inclusion Chemistry in Periodic Mesoporous Hosts, Chem. Mater., 10 (1998) 2950-2963.
[6] K. Moller, T. Bein, Talented Mesoporous Silica Nanoparticles, Chemistry of Materials, 29 (2017) 371-388.
[7] C. Coperet, A. Comas-Vives, M.P. Conley, D.P. Estes, A. Fedorov, V. Mougel, H. Nagae, F. Nunez-Zarur, P.A. Zhizhko, Surface Organometallic and Coordination Chemistry toward Single-Site Heterogeneous Catalysts: Strategies, Methods, Structures, and Activities, Chemical Reviews, 116 (2016) 323-421.
[8] Y. Chen, J.L. Shi, Chemistry of Mesoporous Organosilica in Nanotechnology: Molecularly Organic-Inorganic Hybridization into Frameworks, Advanced Materials, 28 (2016) 3235-3272.
[9] U. Diaz, D. Brunel, A. Corma, Catalysis using multifunctional organosiliceous hybrid materials, Chemical Society Reviews, 42 (2013) 4083-4097.
[10] E.L. Margelefsky, R.K. Zeidan, M.E. Davis, Cooperative catalysis by silica-supported organic functional groups, Chemical Society Reviews, 37 (2008) 1118-1126.
[11] E.J. Acosta, C.S. Carr, E.E. Simanek, D.F. Shantz, Engineering nanospaces: Iterative synthesis of melamine-based dendrimers on amine-functionalized SBA-15 leading to complex hybrids with controllable chemistry and porosity, Advanced Materials, 16 (2004) 985-+.
[12] Q.Q. Wang, V.V. Guerrero, A. Ghosh, S. Yeu, J.D. Lunn, D.F. Shantz, Catalytic properties of dendron-OMS hybrids, Journal of Catalysis, 269 (2010) 15-25.
[13] S. Yoo, J.D. Lunn, S. Gonzalez, J.A. Ristich, E.E. Simanek, D.F. Shantz, Engineering nanospaces: OMS/dendrimer hybrids possessing controllable chemistry and porosity, Chemistry of Materials, 18 (2006) 2935-2942.
[14] J. Han, Y. Lou, X. Cai, B.C. Gibb, D.F. Shantz, Pore Modified FDU-12 as a Novel Container for Dendron Growth, The Journal of Physical Chemistry C, (2017).
[15] J.P.K. Reynhardt, Y. Yang, A. Sayari, H. Alper, Polyamidoamine dendrimers prepared inside the channels of pore-expanded periodic mesoporous silica, Advanced Functional Materials, 15 (2005) 1641-1646.
[16] Q.Q. Wang, D.F. Shantz, Ordered mesoporous silica-based inorganic nanocomposites, Journal of Solid State Chemistry, 181 (2008) 1659-1669.

[17] P.C. Angelome, L.M. Liz-Marzan, Synthesis and applications of mesoporous nanocomposites containing metal nanoparticles, Journal of Sol-Gel Science and Technology, 70 (2014) 180-190.
[18] A. Corma, H. Garcia, Silica-bound homogenous catalysts as recoverable and reusable catalysts in organic synthesis, Advanced Synthesis & Catalysis, 348 (2006) 1391-1412.
[19] M. Perez-Cabero, J. El Haskouri, B. Solsona, I. Vazquez, A. Dejoz, T. Garcia, J. Alvarez-Rodriguez, A. Beltran, D. Beltran, P. Amoros, Stable anchoring of dispersed gold nanoparticles on hierarchic porous silica-based materials, Journal of Materials Chemistry, 20 (2010) 6780-6788.
[20] S. Yoo, S. Yeu, R.L. Sherman, E.E. Simanek, D.F. Shantz, D.M. Ford, Reverse-Selective Membranes formed by Dendrimers on Mesoporous Ceramic Supports, J. Membrane Sci., 334 (2009) 16-24.
[21] J.X. Han, Y.Y. Lou, X.Y. Cai, B.C. Gibb, D.F. Shantz, Pore Modified FDU-12 as a Novel Container for Dendron Growth, Journal of Physical Chemistry C, 121 (2017) 22031-22039.
[22] Y. Lou, D.F. Shantz, Palladium dendron encapsulated nanoparticles grown from MCM-41 and SBA-15, Journal of Materials Chemistry A, 5 (2017) 14070-14078.
[23] R.M. Crooks, M.Q. Zhao, L. Sun, V. Chechik, L.K. Yeung, Dendrimer-encapsulated metal nanoparticles: Synthesis, characterization, and applications to catalysis, Accounts of Chemical Research, 34 (2001) 181-190.
[24] R.W.J. Scott, O.M. Wilson, R.M. Crooks, Synthesis, characterization, and applications of dendrimer-encapsulated nanoparticles, Journal of Physical Chemistry B, 109 (2005) 692-704.
[25] R.W.J. Scott, H. Ye, R.R. Henriquez, R.M. Crooks, Synthesis, Characterization, and Stability of Dendrimer-Encapsulated Palladium Nanoparticles, Chem. Mat., 15 (2003) 3873-3878.
[26] O.M. Wilson, M.R. Knecht, J.C. Garcia-Martinez, R.M. Crooks, Effect of Pd Nanoparticle Size on the Catalytic Hydrogenation of Allyl Alcohol, Journal of the American Chemical Society, 128 (2006) 4510-4511.
[27] L.K. Yeung, R.M. Crooks, Heck Heterocoupling within a Dendritic Nanoreactor, Nano Letters, 1 (2001) 14-17.
[28] M. Zhao, L. Sun, R.M. Crooks, Preparation of Cu Nanoclusters within Dendrimer Templates, Journal of the American Chemical Society, 120 (1998) 4877-4878.
[29] W. Huang, J.N. Kuhn, C.-K. Tsung, Y. Zhang, S.E. Habas, P. Yang, G.A. Somorjai, Dendrimer Templated Synthesis of One Nanometer Rh and Pt Particles Supported on Mesoporous Silica: Catalytic Activity for Ethylene and Pyrrole Hydrogenation, Nano Letters, 8 (2008) 2027-2034.
[30] Y.-G. Kim, S.-K. Oh, R.M. Crooks, Preparation and Characterization of 1−2 nm Dendrimer-Encapsulated Gold Nanoparticles Having Very Narrow Size Distributions, Chem. Mat., 16 (2004) 167-172.
[31] P. Maity, S. Yamazoe, T. Tsukuda, Dendrimer-Encapsulated Copper Cluster as a Chemoselective and Regenerable Hydrogenation Catalyst, ACS Catalysis, 3 (2013) 182-185.
[32] X. Peng, Q. Pan, G.L. Rempel, Bimetallic dendrimer-encapsulated nanoparticles as catalysts: a review of the research advances, Chemical Society Reviews, 37 (2008) 1619-1628.
[33] V.V. Rostovtsev, L.G. Green, V.V. Fokin, K.B. Sharpless, A stepwise Huisgen cycloaddition process: Copper(I)-catalyzed regioselective "ligation" of azides and terminal alkynes, Angewandte Chemie-International Edition, 41 (2002) 2596-+.
[34] C.W. Tornoe, C. Christensen, M. Meldal, Peptidotriazoles on solid phase: [1,2,3]-triazoles by regiospecific copper(I)-catalyzed 1,3-dipolar cycloadditions of terminal alkynes to azides, Journal of Organic Chemistry, 67 (2002) 3057-3064.

[35] H.C. Kolb, M.G. Finn, K.B. Sharpless, Click chemistry: Diverse chemical function from a few good reactions, Angewandte Chemie-International Edition, 40 (2001) 2004-+.
[36] Y. He, Y. Liang, D.J. Wang, The highly sensitive and facile colorimetric detection of the glycidyl azide polymer based on propargylamine functionalized gold nanoparticles using click chemistry, Chem Commun, 51 (2015) 12092-12094.
[37] S. Lee, H. Koo, J.H. Na, S.J. Han, H.S. Min, S.J. Lee, S.H. Kim, S.H. Yun, S.Y. Jeong, I.C. Kwon, K. Choi, K. Kim, Chemical Tumor-Targeting of Nanoparticles Based on Metabolic Glycoengineering and Click Chemistry, Acs Nano, 8 (2014) 2048-2063.
[38] T.N. Jin, M. Yan, Y. Yamamoto, Click Chemistry of Alkyne-Azide Cycloaddition using Nanostructured Copper Catalysts, Chemcatchem, 4 (2012) 1217-1229.
[39] F. Alonso, Y. Moglie, G. Radivoy, Copper Nanoparticles in Click Chemistry, Accounts of Chemical Research, 48 (2015) 2516-2528.
[40] R. Hudson, C.J. Li, A. Moores, Magnetic copper-iron nanoparticles as simple heterogeneous catalysts for the azide-alkyne click reaction in water, Green Chemistry, 14 (2012) 622-624.
[41] S. Jang, Y.J. Sa, S.H. Joo, K.H. Park, Ordered mesoporous copper oxide nanostructures as highly active and stable catalysts for aqueous click reactions, Catalysis Communications, 81 (2016) 24-28.
[42] S. Chassaing, V. Beneteau, P. Pale, When CuAAC 'Click Chemistry' goes heterogeneous, Catalysis Science & Technology, 6 (2016) 923-957.
[43] S.G. Pan, S. Yan, T. Osako, Y. Uozumi, Batch and Continuous-Flow Huisgen 1,3-Dipolar Cycloadditions with an Amphiphilic Resin-Supported Triazine-Based Polyethyleneamine Dendrimer Copper Catalyst, Acs Sustainable Chemistry & Engineering, 5 (2017) 10722-10734.
[44] D. Astruc, D. Wang, C. Deraedt, L.Y. Liang, R. Ciganda, J. Ruiz, Catalysis Inside Dendrimers, Synthesis-Stuttgart, 47 (2015) 2017-2031.
[45] F. Alonso, Y. Moglie, G. Radivoy, M. Yus, Unsupported Copper Nanoparticles in the 1,3-Dipolar Cycloaddition of Terminal Alkynes and Azides, Eur J Org Chem, (2010) 1875-1884.
[46] D.Y. Zhao, Q.S. Huo, J.L. Feng, B.F. Chmelka, G.D. Stucky, Nonionic triblock and star diblock copolymer and oligomeric surfactant syntheses of highly ordered, hydrothermally stable, mesoporous silica structures, Journal of the American Chemical Society, 120 (1998) 6024-6036.
[47] R. He, Y.C. Wang, X.Y. Wang, Z.T. Wang, G. Liu, W. Zhou, L.P. Wen, Q.X. Li, X.P. Wang, X.Y. Chen, J. Zeng, J.G. Hou, Facile synthesis of pentacle gold-copper alloy nanocrystals and their plasmonic and catalytic properties, Nature Communications, 5 (2014).
[48] J. Yin, S.Y. Shan, L.F. Yang, D. Mott, O. Malis, V. Petkov, F. Cai, M.S. Ng, J. Luo, B.H. Chen, M. Engelhard, C.J. Zhong, Gold-Copper Nanoparticles: Nanostructural Evolution and Bifunctional Catalytic Sites, Chemistry of Materials, 24 (2012) 4662-4674.
[49] X. Liu, J. Ruiz, D. Astruc, Prevention of aerobic oxidation of copper nanoparticles by anti-galvanic alloying: gold versus silver, Chem Commun (Camb), (2017).
[50] F. Alonso, Y. Moglie, G. Radivoy, M. Yus, Unsupported Copper Nanoparticles in the 1,3-Dipolar Cycloaddition of Terminal Alkynes and Azides (April, pg 1875, 2010), European Journal of Organic Chemistry, (2010) 5913-5913.
[51] R.E. Schaak, A.K. Sra, Synthesis of atomically ordered nanocrystals from bimetallic nanoparticle precursors., Abstr Pap Am Chem S, 227 (2004) U1537-U1537.